Automated Solder Inspection Method by Means of X-ray Oblique Computed Tomography

Atsushi TERAMOTO*, Takayuki MURAKOSHI*,
Masatoshi TSUZAKA**, Hiroshi FUJITA***

*Nagoya Electric Works Co.,Ltd.
**Department of Radiological Technology, Nagoya University
***Department of Intelligent Image Information,Graduate School of Medicine, Gifu University

ABSTRACT

High-density LSI packages such as ball grid array (BGA) are being utilised in the car electronics and communications infrastructure products. These products require a high-speed and reliable inspection technique for their solder joints. In this paper, we propose an automated X-ray inspection technique for BGA mounted substrate based on oblique computed tomography (OCT). Automated inspection consists of OCT capturing, position adjustment, bump extraction, character extraction and judgment. We proposed five characteristic features related to the bump shape. Moreover, by combining the characteristic features using artificial neural network, the condition of a solder bump was determined. In the experiments, we evaluate these techniques using actual BGA-mounted substrate. As a result, the correct rate of judgment reached 99.7%, which shows the clearly indicates that our method may be useful in the practice.

Index Terms— X-ray, CT, BGA, Bump, Inspection

1. INTRODUCTION

High density LSI packages such as ball grid array (BGA) package [1] are being utilized on substrates in not only consumer products such as mobile phones and personal computers but also in products that require high reliability, such as car electronics and communication infrastructure systems. The electrical junction of the BGA is formed by solder bumps that are placed in a grid-like formation under the LSI package. Therefore, the solder shape of a BGA cannot be observed by optical techniques. X-ray inspection is a suitable technique for the non-destructive inspection of internal conditions such as the solder shape. Since the advent of the BGA package, X-ray inspection has been widely used as the inspection method for BGA-mounted substrates in consumer electronic products [2]–[4]. X-ray fluoroscopy is suitable for the fast inspection of consumer products because it employs simple mechanics and is able to obtain 2D information from the detector instantaneously. However, the X-ray fluoro-scopic image is a projection image, and the information in it is compressed along the z direction. Therefore, an inspection based on 3D shape infor-mation is required for the accurate inspection of solder joints.

Some teams proposed the use of laminography which generates a slice image by a synchronized motion between the X-ray source and the detector [5]-[7]. This technique emphasizes the soldering plane and shades the plane that is not in the focus. The laminography technique provides faster inspection because calculations are not required. However, the spatial resolution is low and there is scope for improving it in order to offer precise inspection of BGA solder joints.

To obtain the accurate 3D shape of a solder joint, we proposed a high-speed oblique computed tomography (OCT) system for manufacturing processes [8]. OCT obtains the projection images of an object from an oblique direction by rotating the X-ray detector. When we apply OCT to the inspection of a BGA-mounted substrate, the X-ray detector moves horizontally when scanning; thin and wide objects such as the substrate do not touch the X-ray generator and detector. Therefore, although the substrate may be close to the X-ray generator, we can obtain a 3D image with high magnification without cutting the substrate. Currently, OCT is being used in more than ten factories for BGA mounting, and skilled inspectors examine the condition of solder junctions by viewing the OCT image. Manual inspection is more adaptable as compared to automated inspection. However, we have to be concerned about the inspection of heavy loads and the fluctuation of inspection sensitivity for soldering defects. Therefore, the establishment of an automated inspection method for the inspection of soldering joints of BGA packages using OCT images is required urgently.

In this paper, we propose a new automated inspection method for the soldering of BGA packages by using OCT images. Automated inspection consists of OCT capturing, position adjustment, bump extraction, character extraction, and judgment. We employ five characteristic features that are related to the soldering condition. Furthermore, inferences are drawn considering these characteristic features using artificial neural network. We evaluate this technique through the experiment using actual BGA-mounted substrate.

2. AUTOMATED INSPECTION PROCESSING

2.1 Inspection Outline

Automated inspection consists of 1) OCT capture, 2) Position adjustment, 3) Bump extraction, 4) Character extraction, and 5) Judgment. Details are described as follows.

2.2 OCT Capturing

The structure of the OCT system [8] is shown in Fig.1. The system consists of a rotational flat panel detector (FPD), an X-Y stage and an open-type X-ray generator. The FPD and the sample rotate simultaneously, and X-ray projection images are obtained from various directions. Unlike the conventional axial CT, the X-ray generator need not rotate because the radiation angle is as wide as 130°. The light weight of the FPD results in a low mechanical load; this further allows high-speed scanning. The geometrical magnification increases as the distance between a sample and the X-ray generator decreases. The geometrical magnification of our OCT prototype is 200, and a spatial resolution of 0.25 μm is attained. The X-ray generator and the FPD do not interfere because the direction of the X-ray radiation is inclined. It is the most advantageous in OCT that cut out of inspect region is not needed. The X-ray projection images are transferred to the host memory via an image grabber, and the OCT image is obtained by performing 3D reconstruction. The matrix size of our OCT prototype is 2048 × 2048 × 64 pixels; the reconstruction is performed while correcting the projection image. Figs.2 and 3 show the OCT images. In Fig.2 (b), the bump outline at the defective bump is unclear, which indicates that the solder is not connected correctly between the bump and the substrate. Additionally, Fig.3 also indicates that soldering is defective on the substrate side.

2.3 Position adjustment

The BGA-mounted substrate has warpage which is developed during the manufacturing and the reflow process. The fluctuation of the inspection position due to the warpage causes the degradation of the performance in the case of 3D inspection. In order to correct the warpage of substrate, we introduced the laser displacement sensor placed at the back side of the substrate, and the distances from the sensor to the substrate are measured. More than 3 positions are measured, the equation of the least square plane, $z = ax + by + c$, was obtained by using the values of the measured distances. After obtaining the equation of the plane, the OCT image was tilted based on the coefficients a and b; thus, the warpage was corrected. Moreover, the shift in the z direction was corrected by the coefficient c. Fig.4 shows the result of the correction performed for the OCT image. The original image in Fig.4(a), the right side of the image becomes obscure if the substrate is tilted. On the other hand, all the bumps can be observed for the same condition in the corrected image shown in Fig.4(b); it was confirmed that the correction works well.

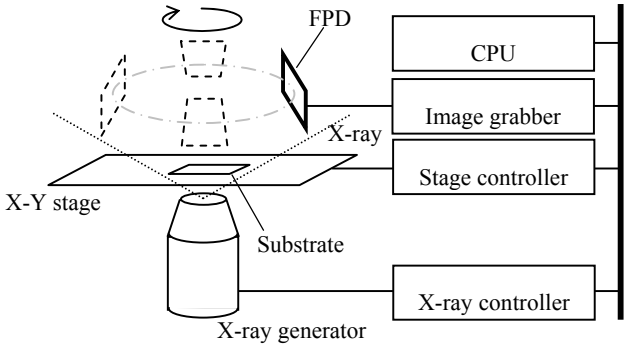

Fig.1 Structure of OCT system

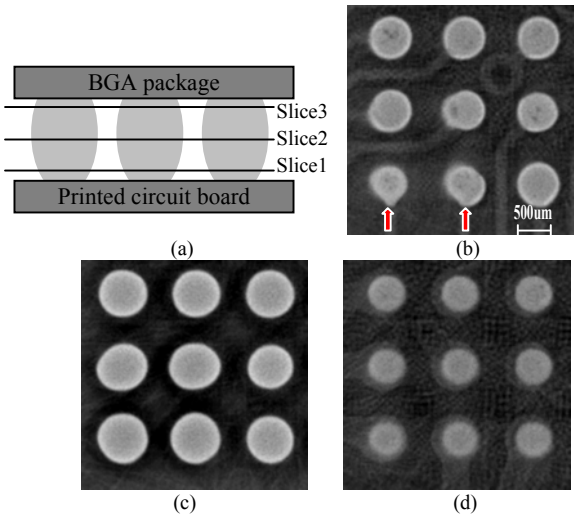

Fig.2 (a) illustration of the cross-sectional view of the BGA-mounted substrate and the slice position. (b)–(d) horizontal slice image at slice positions 1–3, respectively.

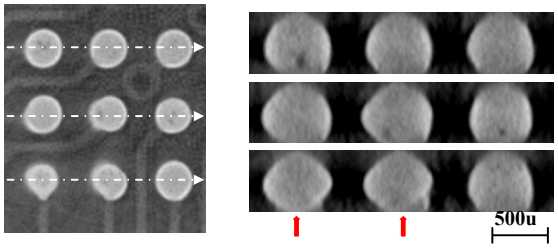

Fig.3 (a) horizontal slice image which gives the slice line for the vertical slice. (b) vertical slice images along the white lines in (a).

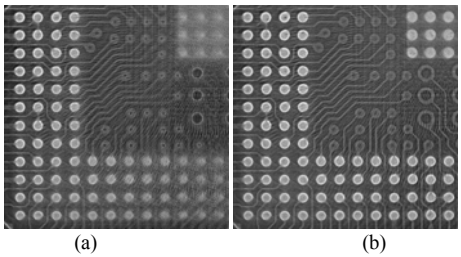

Fig.4 (a) original image. (b) corrected image.

2.4 Automated extraction of solder bump

In order to extract the bump region, binarization is applied to the corrected 3D OCT image. OCT image has many artifacts because not only because the OCT system generates images from a small number of projections (32–64) but also because of the effect of artifacts due to the incomplete information in the OCT system. As a result, the threshold of binarization has to be changed for each visual field. In this study, the threshold of binarization is calculated automatically by using the p-tile method [9], and only the bump region is extracted.

2.5 Character extraction

When a soldering defect occurs, following phenomena are observed: decrease of sectional area, increase in the center of gravity, distortion of the sectional shape, decrease in the sharpness of the bump outline and increase in the curvature. In this study, we introduce the following five characteristic features related to the above-mentioned phenomena.

A. The ratio of bump sectional area: BAR

$$BAR = BA(h_1) / BA(h_2) \quad (1)$$

B. The center of the gravity: BG

$$BG = \frac{\sum_i BA(i) \cdot i}{\sum_i BA(i)} \quad (2)$$

C. Bump flatness: BF

$$BF = \frac{R_{\max}}{2 \cdot \sqrt{BA(h_1)/\pi}} \quad (3)$$

D. Total amount of bump edges: BE

$$BE = \sum_x \sum_y E(x, y) \quad (4)$$

E. Bump curvature: BC

BC is the curvature which is calculated from the bump radiuses at $z = h_1 - 1$, $z = h_1$, and $z = h_1 + 1$.

Where h_1 and h_2 are the z position of solder junction near the substrate and center of bump, respectively. $BA(x)$ is the sectional area at $z = x$, R_{max} is the maximum diameter of bump, and $E(x,y)$ is the edge extracted image.

2.6 Judgement

The multiple characteristic features calculated in the previous section are shown as feature vector $\boldsymbol{x} = (x_1, x_2, x_3, \cdots, x_n)^T$. The aim of this study is to determine whether the feature vector considers every bump and to distinguish the bumps that are good and defective. In this study, we focused on artificial neural network (ANN) as a judgment method [10]. We employed feed forward ANN, as shown in Fig.5. The structure of an ANN consists of an input layer, hidden layer and output layer. The characteristic features are given to the input layer, and the judgment result is obtained from the output layer. The ANN constructs the input-output relation by "learning" processing. The learning processing is carried out before the inspection; the number of input and teaching data that correspond to the input data are prepared. The ANN is trained by means of a learning algorithm such as back propagation method. In this study, the ANN has one output layer—0 given in case of a good bump and 1 is given for a defective one. In the inspection phase, the characteristic features are provided to the input layer of the ANN, and the bump is judged as good when the output value is less than 0.5 and as defective when the output is greater than 0.5.

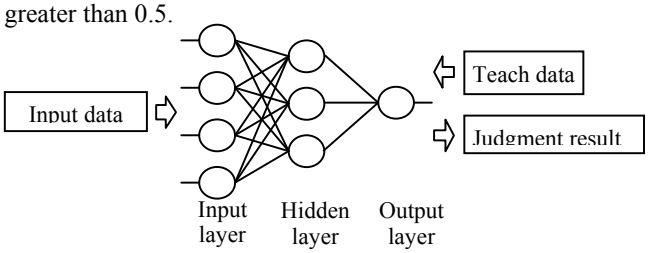

Fig.5 Structure of ANN for judgment

3. EXPERIMENTS

In order to verify the effectiveness of this technique, an automated inspection was carried out using a BGA-mounted substrate. Table 1 contains the description of the inspection sample and inspection parameters. The number of bumps was 350, and all bumps were classified as good or defective by viewing the OCT images. OCT image was generated using 32 projections per scan. By parallelizing the collection of projection image and reconstruction processing, the generation of the OCT image finished in 32 seconds per scan. The judgment of solder bump was performed using the ANN. It consisted of five units for the input layer, five units for the hidden layer and one unit for the output layer. A linear function was used as the input/output function for the output layer. The number of learning iterations was 10000; quasi-Newton method [11] was used as the learning method. The 344 bumps were randomly divided into five-data sets, the evaluation by the cross validation method was carried out.

The histogram of the output value of the ANN is shown in Fig.6. One bump is judged as defective among the good ones; however, the other bumps are judged correctly. We checked the only bump that was misjudged. It was difficult to judge that bump as it was connected at an area between the substrate and the bump.

Table 2 is the summarized result of the judgment performance for ANN and some characteristic features in which there are deviations in the distribution of the good and defective bumps. Since the distribution of good and defective bumps overlapped for a single characteristic feature, we set the boundary where the distribution crosses and counted the number of accurately judged bumps.

The result for the ANN reached 99.7%, while the largest correct rate was 92% for the single characteristic features.

These results showed that a good judgment ability was

obtained by combining multiple characteristic features.

Next, a test case using the proposed technique is shown in Fig.7 and Table 3. Bump Nos.1 and 2 are defective; their *BAR* and *BE* are smaller than those of the good ones. Suitable outputs were also obtained by using the ANN.

TABLE 1 INSPECTION SAMPLE AND PARAMETERS

Parameter name	Value
Bump diameter [μm]	600
The total number of bumps	350
The number of good bumps	291
The number of defective bumps	59
X-ray voltage [kV]	100
X-ray focal spot size [μm]	1.0
Geometric magnification	8.3
Projection pitch [degree]	11.25
Image matrix size (X × Y × Z)	1024 × 1024 × 100

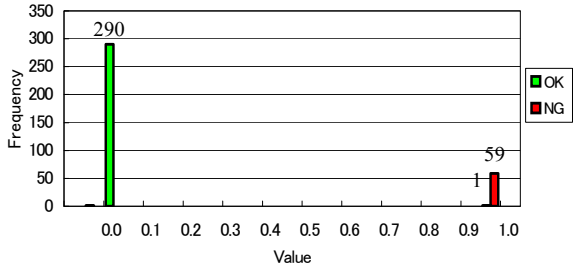

Fig.6 Histogram of the output of ANN.

TABLE 2 SUMMARY OF EVALUATION RESULT

	The number of miss judgment in NG bump	The number of miss judgment in OK bump	Correct rate [%]
BAR	4	7	96.8
BG	12	15	92.2
BE	10	3	96.2
ANN	0	1	99.7

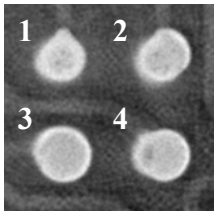

Fig.7 Example image of automated inspection. Label numbers correspond to the result in Table 3.

TABLE 3 INSPECTION RESULT

Number	*BAR*	*BG*	*BF*	*BC*	*BE*	*ANN*
1 (NG)	0.70	49.8	1.044	0.037	1.23E+08	1.00
2 (NG)	0.75	48.7	1.059	0.034	2.22E+08	0.99
3	0.85	47.4	1.056	0.030	2.82E+08	0.00
4	0.79	47.2	1.047	0.033	2.51E+08	0.00

4. CONCLUSION

In this paper, the automated inspection technique using OCT for soldered joints of BGA mounted substrate was newly proposed. In this technique, the bump region was firstly extracted from the OCT image and several characteristic features were calculated from the region. Moreover, the condition of each solder bump was determined by combining the characteristic features using artificial neural network. In the experiments, we evaluated these techniques by using actual BGA-mounted substrates. As a result, the correct judgement rate reached 99.7%, and we confirmed that our method was able to distinguish between good and defective soldering bumps. We will apply this method to actual OCT systems that operate in manufacturing processes in order to confirm the effectiveness of this method.

5. REFERENCES

[1] R.Ghaffarian, "BGAs for high reliability applications," Electronics Packaging & Production, Vol. 38, No.3, pp.45-52, 1998.

[2] D.Geiger and D.Shangguan, "X-ray Inspection of Area Array Packages Using Tin-Lead and Lead-Free Solders," The Proc. of SMTA, Chicago, pp.26-30, 2004.

[3] A.Teramoto, T.Murakoshi, M.Tsuzaka, H.Fujita, "Development of an automated X-ray inspection method for microsolder bumps," Proc. of EMAP, pp. 21-26, 2005.

[4] A.Teramoto, T.Murakoshi, M.Tsuzaka, and H.Fujita, "Automated X-ray inspection method for fillet-less mounted chip components," IEEJ Trans. of TEEE, letter, in press.

[5] G. Leinbach and S. Rooks, "Process variation evaluation via X-ray laminography," Surface Mount Technology, pp. 38-40, 1995.

[6] S.M.Rooks, B.Benhabib, and K.C.Smith, "Development of an inspection process for ball-grid-array technology using scanned-beam X-ray laminography," IEEE Trans. Comp., Packag., Manufact. Technol., vol. 18, no.3, pp.851-861, 1995.

[7] V.Sankaran, A.R.Kalukin, and R.P.Kraft, "Improvements to X-Ray Laminography for Automated Inspection of Solder Joints", IEEE Trans. Comp., Packag., Manufact. Technol., vol.21, no.2, pp.148-154, 1998.

[8] A.Teramoto, T.Murakoshi, M.Tsuzaka, H.Fujita, "High Speed Oblique X-ray CT System for Printed Circuit Board," IEEJ Trans. of TEEE, submitting.

[9] W.Doyle, "Operations useful for similarity-invariant pattern recognition," Journal of the ACM, vol.9, no.2, pp.259-267, 1962.

[10] D.E.Rumelhart, J.L.McClelland and the PDP research group, "Parallel Distributed Processing," vol.1 and 2, MIT Press, Cambridge, 1986.

[11] R.Battiti, "First and second order methods for learning: Between steepest descent and Newton's method," Neural Computation, vol. 4, no. 2, pp. 141-166, 1992.